ORGANOMETALLICS

Article

pubs.acs.org/Organometallics

Heterolytic Cleavage of Dihydrogen by an Iron(II) PNP Pincer Complex via Metal−Ligand Cooperation

Bernhard Bichler,[†] Christian Holzhacker,[†] Berthold Stöger,[§] Michael Puchberger,[‡] Luis F. Veiros,[∥] and Karl Kirchner*[,†]

[†]Institute of Applied Synthetic Chemistry, [‡]Institute of Materials Chemistry, and [§]Institute of Chemical Technologies and Analytics, Vienna University of Technology, Getreidemarkt 9, A-1060 Vienna, Austria

[∥]Centro de Química Estrutural, Instituto Superior Técnico, Universidade Técnica de Lisboa, Av. Rovisco Pais No. 1, 1049-001 Lisboa, Portugal

Supporting Information

ABSTRACT: The bis-carbonyl Fe(II) complex *trans*-[Fe(PNP-*i*Pr)(CO)$_2$Cl]$^+$ reacts with Zn as reducing agent under a dihydrogen atmosphere to give the Fe(II) hydride complex *cis*-[Fe(PNP-*i*Pr)(CO)$_2$H]$^+$ in 97% isolated yield. A crucial step in this reaction seems to be the reduction of the acidic NH protons of the PNP-*i*Pr ligand to afford H_2 and the coordinatively unsaturated intermediate [Fe(PNP^H-*i*Pr)(CO)$_2$]$^+$ bearing a dearomatized pyridine moiety. This species is able to bind and heterolytically cleave H_2 to give *cis*-[Fe(PNP-*i*Pr)(CO)$_2$H]$^+$. The mechanism of this reaction has been studied by DFT calculations. The proposed mechanism was supported by deuterium labeling experiments using D_2 and the N-deuterated isotopologue of *trans*-[Fe(PNP-*i*Pr)(CO)$_2$Cl]$^+$. While in the first case deuterium was partially incorporated into both N and Fe sites, in the latter case no reaction took place. In addition, the N-methylated complex *trans*-[Fe(PNP^{Me}-*i*Pr)(CO)$_2$Cl]$^+$ was prepared, showing no reactions with Zn and H_2 under the same reaction conditions. An alternative synthesis of *cis*-[Fe(PNP-*i*Pr)(CO)$_2$H]$^+$ was developed utilizing the Fe(0) complex [Fe(PNP-*i*Pr)(CO)$_2$]. This compound is obtained in high yield by treatment of either *trans*-[Fe(PNP-*i*Pr)(CO)$_2$Cl]$^+$ or [Fe(PNP-*i*Pr)Cl$_2$] with an excess of NaHg or a stoichiometric amount of KC_8 in the presence of carbon monoxide. Protonation of [Fe(PNP-*i*Pr)(CO)$_2$] with HBF_4 gave the hydride complex *cis*-[Fe(PNP-*i*Pr)(CO)$_2$H]$^+$. X-ray structures of both *cis*-[Fe(PNP-*i*Pr)(CO)$_2$H]$^+$ and [Fe(PNP-*i*Pr)(CO)$_2$] are presented.

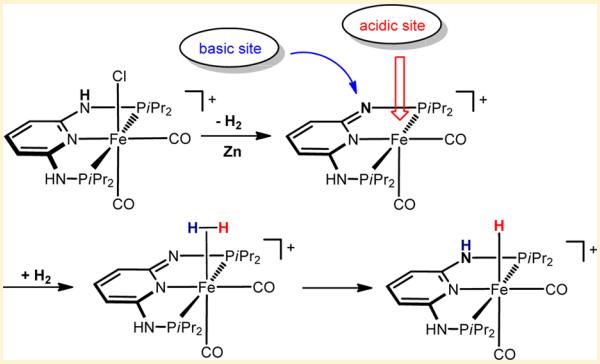

INTRODUCTION

An interesting way of bond activation by metal−ligand cooperation involves aromatization/dearomatization of the ligand in pincer-type complexes.[1,2] In particular, pincer ligands in which a central pyridine-based backbone is connected with −CH_2PR_2 and/or CH_2NR_2 substituents were shown to exhibit this behavior.[3] This has resulted in the development of novel and unprecedented transition-metal chemistry under both stoichiometric[4] and catalytic[5] conditions involving, for instance, H−H, O−H, N−H, and C−H bond activation. Very recently, Milstein and co-workers also discovered highly efficient pyridine-based PNP pincer iron complexes that catalyze hydrogenation of ketones to alcohols and hydrogenation of CO_2 to formate salts,[6] where this type of cooperation plays a key role in the heterolytic cleavage of H_2. In general, splitting of a highly acidic coordinated H_2 ligand in a fashion that a proton is accepted by an external or, more efficiently, by an internal Lewis base X (where X can be N, O, S, C, etc. donors) to leave a hydride ligand on the metal center has been extensively studied in recent years (Scheme 1).[7]

Scheme 1

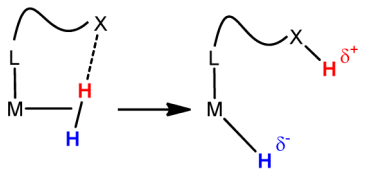

We have recently begun to investigate the transition-metal chemistry of PNP ligands based on 2,6-diaminopyridine where, in contrast to the above PNP pincer ligands, the central pyridine ring contains −$NHPR_2$ substituents in the two ortho positions. The more acidic NH spacer may favor the dearomatization step and thus offer unusual and interesting reactivities. Thus far, we reported on the synthesis and reactivity of several Ni(II), Pd(II), Pt(II), Mo(0), Mo(II),

Received: March 21, 2013
Published: July 26, 2013

   dx.doi.org/10.1021/om400241x | *Organometallics* 2013, 32, 4114−4121

Ru(II), and Fe(II) PNP complexes.[8−11] Most recently, Huang and co-workers described the use of Ru(II) complexes with these types of PNP ligands as efficient base-free catalysts for the transfer hydrogenation of ketones.[12] In the course of our investigations we observed that a reversible aromatization/dearomatization reaction, a prerequisite for heterolytic H−H activation, could be achieved in dicationic Fe(II) PNP complexes. In fact, treatment of [Fe(PNP-BIPOL)-$(CH_3CN)_3]^{2+}$ with an excess of NaHg (3%) as reducing agent resulted in an immediate evolution of H_2 gas, affording the deprotonated dearomatized monocationic complex [Fe-(PNP-BIPOL)$(CH_3CN)_3]^+$ as shown in Scheme 2. This

Scheme 2

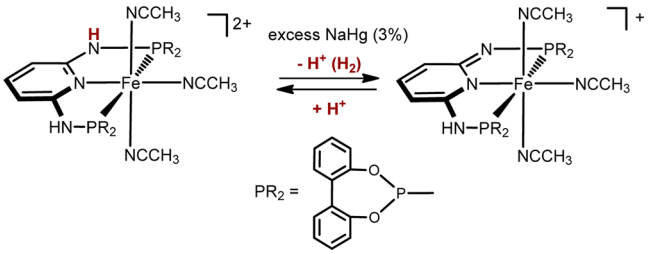

complex was even characterized by X-ray crystallography. The deprotonation was reversible, and addition of HBF_4 to a solution of [Fe(PNP-BIPOL)$(CH_3CN)_3]^+$ cleanly afforded the dicationic complex where the pyridine ring regained full aromaticity.

In an effort to broaden the scope of this concept for the preparation of novel cooperative iron-based PNP catalysts, we report herein the synthesis of the new Fe(II) hydride PNP pincer complex *cis*-[Fe(PNP-*i*Pr)$(CO)_2H]^+$, which is formed in an unexpected manner involving heterolytic hydrogen cleavage. Moreover, an alternative method via selective protonation of the Fe(0) complex [Fe(PNP-*i*Pr)$(CO)_2$] is presented. X-ray structures of both *cis*-[Fe(PNP-*i*Pr)$(CO)_2H]^+$ and [Fe(PNP-*i*Pr)$(CO)_2$] are given.

RESULTS AND DISCUSSION

In an attempt to obtain the Fe(0) complex [Fe(PNP-*i*Pr)$(CO)_2$], the bis-carbonyl Fe(II) complex *trans*-[Fe(PNP-*i*Pr)$(CO)_2Cl]^+$ (**1**, as the SbF_6^- salt) was treated with Zn as reducing agent at room temperature in solvents such as THF, toluene, and dioxane for 2 h. Surprisingly, instead of the expected Fe(0) complex the Fe(II) monohydride *cis*-[Fe(PNP-*i*Pr)$(CO)_2H]^+$ (**5**) was obtained in 40% isolated yield together with several intractable materials (Scheme 3). The formation of this species was independent of whether deuterated or nondeuterated solvents were used: e.g., THF-d_8, toluene-d_8, and dioxane-d_8. If, on the other hand, **1** was reacted with Zn under a dihydrogen atmosphere (1 bar), **5** was afforded in 97% isolated yield. This seems to suggest that in the first case the hydride ligand solely originates from the acidic NH protons of the PNP ligand which are reduced to H_2 with concomitant formation of Zn^{2+} ions. The latter act additionally as chloride scavengers. This type of reaction has precedence in iron PNP pincer chemistry (Scheme 2).[8]

IR and NMR monitoring of the reaction of **1** with Zn in THF-d_8 revealed that the formation of **5** proceeds via the bis-carbonyl intermediate *cis*-[Fe(PNP-*i*Pr)$(CO)_2Cl]^+$ (**4**), as shown in Scheme 3. It has to be noted that the isomerization of **1** to **4** takes place only to some extent and these species are apparently in equilibrium with one another. Accordingly, under these conditions isolation of pure **4** was not possible.[13] While **1** exhibits a single ν_{CO} band at 2013 cm^{-1}, **4** displays the expected two signals of the symmetric and asymmetric CO stretching frequencies at 2050 and 2001 cm^{-1}. In the $^{31}P\{^1H\}$ NMR **1** exhibits a singlet at 118.5 ppm, whereas the *cis*-CO complex **4** gives rise to a singlet at 134.2 ppm. Characteristic features in the $^{13}C\{^1H\}$ NMR spectrum of **4** are two low-field triplet resonances centered at 209.4 (J_{CP} = 17.4 Hz) and 208.4 ppm (J_{CP} = 22.7 Hz) assignable to the carbonyl carbon atoms *trans* and *cis* to the pyridine nitrogen, respectively. The starting material **1** displays only one triplet for the two CO carbon atoms centered at 211.6 ppm (J_{CP} = 24.4 Hz).

Complex **5** is a thermally robust pale yellow solid that is air stable in the solid state but slowly decomposes in solution.

Scheme 3

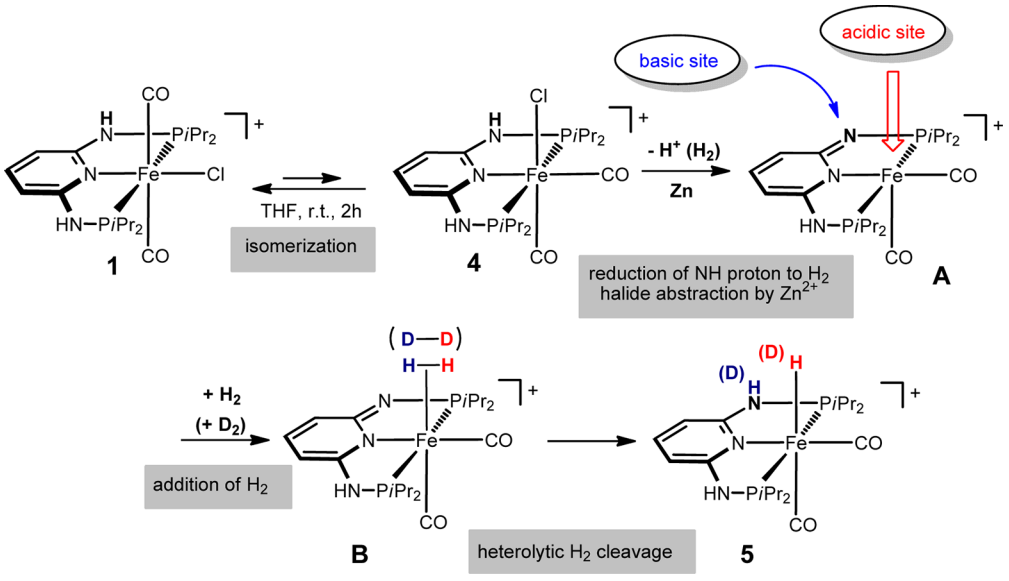

dx.doi.org/10.1021/om400241x | *Organometallics* 2013, 32, 4114−4121

Characterization was accomplished by elemental analysis and by ^{1}H, $^{13}C\{^{1}H\}$, and $^{31}P\{^{1}H\}$ NMR and IR spectroscopy. The ^{1}H NMR spectrum confirmed the presence of one hydride ligand, which appeared at −7.47 ppm as a well-resolved triplet with a $^{2}J_{HP}$ coupling constant of 47.7 Hz. In the $^{13}C\{^{1}H\}$ NMR spectrum the most noticeable resonances are the two low-field resonances of the carbonyl carbon atoms *trans* and *cis* to the pyridine nitrogen observed as two triplets centered at 212.2 (J_{CP} = 20.2 Hz) and 207.5 ppm (J_{CP} = 11.8 Hz), respectively. The $^{31}P\{^{1}H\}$ NMR spectrum of complex **5** gives rise to a singlet at 162.8 ppm. In the IR spectrum the two bands for the symmetric and asymmetric CO stretching frequencies are found at 2027 and 1969 cm^{-1}.

In addition to the spectroscopic characterization, the solid-state structure of **5** was determined by single-crystal X-ray diffraction. A structural view is depicted in Figure 1 with

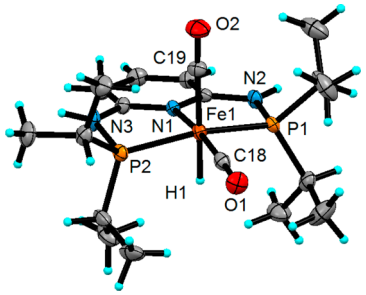

Figure 1. Structural view of *cis*-[Fe(PNP-*i*Pr)$(CO)_2$H]SbF_6 (**5**) showing 50% thermal ellipsoids (SbF_6^- counterion omitted for clarity). Selected bond lengths (Å) and angles (deg): Fe1−P1 = 2.198(2), Fe1−P2 = 2.112(2), Fe1−N1 = 2.007(3), Fe1−C18 = 1.752(4), Fe1−C19 = 1.811(3), Fe1−H1 = 1.45(2); P1−Fe1−P2 = 159.76(4), C18−Fe1−C19 = 97.6(2), N1−Fe1−C18 = 171.4(2), Fe1−C18−O1 = 177.1(3), Fe1−C19−O2 = 177.0(3).

selected bond distances given in the caption. Complex **5** adopts a distorted-octahedral geometry around the metal center with the hydride ligand being in a position *trans* to a CO ligand. The PNP ligand is coordinated to the iron center in a typical tridentate meridional mode, with a P1−Fe1−P2 angle of 159.76(4)°. The Fe−C bond of the CO ligand *trans* to the pyridine nitrogen of the PNP ligand is slightly shorter than that *cis* to the PNP moiety, due to the stronger *trans* influence of the hydride in comparison to that of the pyridine ligand, being 1.752(4) and 1.811(3) Å. The hydride and the N−H atoms could be unambiguously located in the difference Fourier maps. The Fe−H distance was restrained to 1.46(2) Å.

A reasonable mechanism which accounts for the formation of *cis*-[Fe(PNP-*i*Pr)$(CO)_2$H]$^+$ (**5**) is proposed in Scheme 3. Upon partial isomerization of *trans*-[Fe(PNP-*i*Pr)$(CO)_2$Cl]$^+$ (**1**) to the thermodynamically more stable isomer *cis*-[Fe(PNP-*i*Pr)$(CO)_2$Cl]$^+$ (**4**), reduction of the acidic NH protons of the PNP-*i*Pr ligand by Zn results in the release of H_2 and concomitant formation of Zn^{2+} ions. The latter act as halide scavengers, abstracting the chloride ligand, and the coordinatively unsaturated cationic 16e complex [Fe(PNP^H-*i*Pr)$(CO)_2$]$^+$ (**A**) is formed. This step is also accompanied by dearomatization of the pyridine moiety. This species readily binds H_2 and yields [Fe(PNP^H-*i*Pr)$(CO)_2(\eta^2$-$H_2)$]$^+$ (**B**). Heterolytic cleavage of the coordinated and thus activated H_2 ligand finally results in the formation of the hydride complex **5**.

In order to obtain further evidence for the proposed mechanism, several experiments, including deuterium-labeling studies, were performed under the same reaction conditions. Broad deuteride and N−D signals were observed in the ^{2}H NMR spectrum when D_2 was used in place of H_2 due to the formation of the corresponding isotopologue of **5**, giving rise to deuterium resonances at 6.0 (N−D) and −7.5 ppm (Fe−D). The yield was lower, being about 75% apparently due to a kinetic isotope effect (KIE), indicating that a H−H cleavage process is involved in the rate-determining step (vide infra). Increasing the reaction time from 2 to 4 h afforded **5** in 95% yield. Moreover, the isotopologue **1-d$_2$**, featuring N−D instead of N−H moieties, did not afford **5** under the same reaction conditions (Scheme 4), pointing to a large KIE for the N−D

Scheme 4

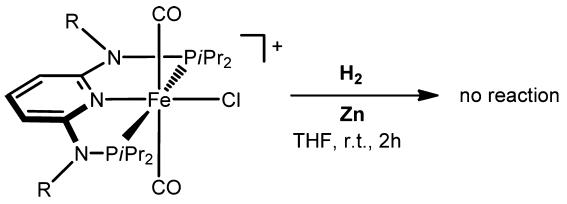

R = D (**1-d$_2$**)
R = Me (**6**)

bond cleavage under reductive conditions. Such observations are not uncommon for reactions involving proton-coupled electron transfer.[14] Finally, as anticipated, also the N-methylated complex *trans*-[Fe(PNP^{Me}-*i*Pr)$(CO)_2$Cl]$^+$ (**6**) did not react with Zn in the absence or presence of H_2 (Scheme 4). Accordingly, all these experiments strongly favor our mechanistic proposal of an involvement of the acidic N−H protons of the PNP ligand and the iron center: i.e., metal−ligand cooperation.

The addition of H_2 to the intermediate [Fe(PNP^H-*i*Pr)$(CO)_2$] (**A**) was also investigated by means of DFT calculations.[15] The free energy profile obtained is presented in Figure 2. Starting with the separated reactants, there is formation of a van der Waals pair between the two reacting molecules, H_2 and [Fe(PNP^H-*i*Pr)$(CO)_2$]$^+$ (**A**), with a rather long Fe−H_2 distance (5.67 Å), and a correspondingly small stabilization of the system (3.9 kcal mol^{-1}). From here, [Fe(PNP^H-*i*Pr)$(CO)_2(\eta^2$-$H_2)$]$^+$ (**B**) is formed in a single step, going over a negligible energy barrier (0.7 kcal mol^{-1}). In the corresponding transition state, **TS$_{AB}$**, coordination of the dihydrogen molecule is only incipient with rather long Fe−H distances (2.83 and 3.18 Å) and an H−H bond length (0.74 Å) equal to that existing in free H_2. In the final step of the mechanism, from **B** to **5**, splitting of the H−H bond occurs with formation of the Fe−H hydride and protonation of the neighboring imine N atom. In the transition state **TS$_{B4}$** the cleavage of the H−H bond is well advanced, as shown by a distance of 0.92 Å, and there is a considerable distortion in the geometry of the PNP ligand in order for the imine N atom to approach the incoming proton. Thus, in **TS$_{B4}$**, the pyridine ring is rotated with respect to the plane of the PNP ligand by an angle of 21°,[16] bringing the incoming proton and the N atom to a distance of only 1.55 Å. The last step is the rate-limiting step of the path, with a calculated barrier of 22.8 kcal mol^{-1}, denoting a viable reaction.

Finally, the synthesis of the Fe(0) complex [Fe(PNP-*i*Pr)$(CO)_2$] (**7**) was achieved by stirring either *trans*-[Fe(PNP-

dx.doi.org/10.1021/om400241x | *Organometallics* 2013, 32, 4114−4121

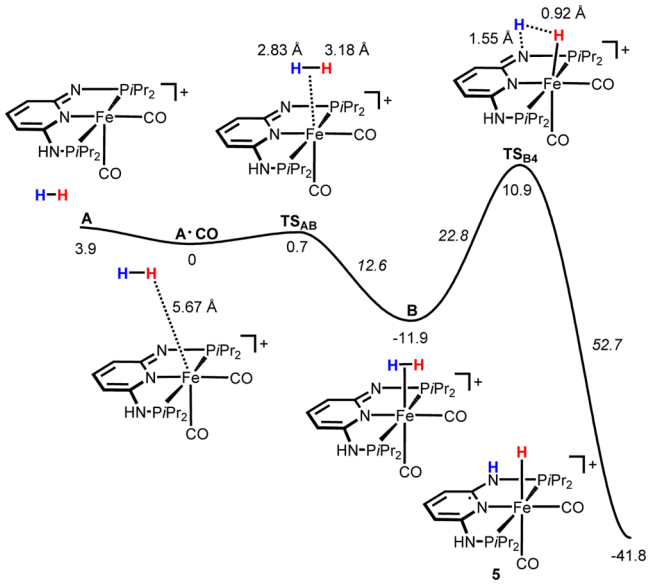

Figure 2. Free energy profile (kcal/mol) for the intramolecular heterolytic dihydrogen cleavage and formation of octahedral *cis*-$[Fe(PNP\text{-}iPr)(CO)_2H]^+$ (**5**). Values in italics correspond to barriers, and the relevant distances (Å) are indicated.

*i*Pr)$(CO)_2Cl]^+$ (**1**) or $[Fe(PNP\text{-}iPr)Cl_2]$ (**2**) in THF with an excess of NaHg (5%) or a stoichiometric amount of KC_8 in the presence of carbon monoxide (Scheme 5). This compound was obtained in 95% isolated yield as an air-sensitive but thermally stable orange solid. The identity of this complex was unequivocally established by ^1H, $^{13}C\{^1H\}$, and $^{31}P\{^1H\}$ NMR and IR spectroscopy and elemental analysis.

In the IR spectrum of **7** in THF, two intense carbonyl bands were observed at 1866 and 1816 cm^{-1}. For comparison, in the related Fe(0) complexes $[Fe(PNP^{CH2}\text{-}iPr)(CO)_2]$ (PNP^{CH2}-*i*Pr = bis(diisopropylphosphinomethyl)pyridine)[17] these bands were found at 1842 and 1794 cm^{-1}. The shift of the CO bands to somewhat higher frequencies is consistent with a less reducing Fe(0) center in **7** in comparison to $[Fe(PNP^{CH2}\text{-}iPr)(CO)_2]$, which is apparently the stronger π base to the coordinated CO. In the $^{13}C\{^1H\}$ NMR spectrum at −80 °C the CO ligand gives rise to a low-field resonance triplet centered at 219.5 ppm with a coupling constant J_{CP} of 27.8 Hz. It has to be noted that, at room temperature, the CO signal was broad. In the $^{31}P\{^1H\}$ NMR spectrum a singlet at 173.8 ppm is observed.

The molecular structure of **7** was determined by X-ray crystallography. A structural view is depicted in Figure 3, with

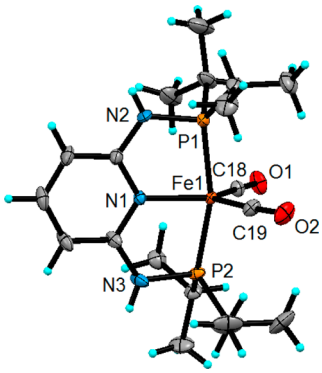

Figure 3. Structural view of $[Fe(PNP\text{-}iPr)(CO)_2]\cdot CH_2Cl_2$ (**7**·CH_2Cl_2) showing 50% thermal ellipsoids (CH_2Cl_2 omitted for clarity). Only one of the two crystallographically independent complexes is shown.

selected bond distances and angles reported in Table 1. The overall geometry about the iron center is best described as distorted trigonal bipyramidal. For comparison, the related complexes $[Fe(PNP^{CH2}\text{-}iPr)(CO)_2]$[15] (Table 1) and $[Fe(PhP\text{-}[CH_2CH_2CH_2P(OiPr)_2]_2)(CO)_2]$[18] adopt an almost perfect trigonal-bipyramidal geometry, while the bulkier complex $[Fe(PNP^{CH2}\text{-}tBu)(CO)_2]$ (PNP^{CH2}-*t*Bu = bis(di-*tert*-butylphosphinomethyl)pyridine)[19] has an unusual square-pyramidal structure. In complex **7**, the two carbonyl ligands and the pyridine nitrogen define the equatorial plane with bond angles of 113.88(9), 127.45(7), and 118.67(7)° for C18−Fe1−C19, N1−Fe1−C18, and N1−Fe1−C19, respectively. A significant distortion is observed in the axial phosphine ligands, where the P1−Fe1−P2 bond angle of 163.01(3)° is contracted toward the pyridine ring. Moreover, one of the two Fe−C−O angles deviates significantly from linearity, with Fe1−C19−O2 and Fe1−C18−O1 being 169.24(16) and 175.47(15)°, respectively. The corresponding angles Fe2−C37−O3 and Fe2−C38−O4 of the crystallographically independent second complex are slightly larger, being 172.72(15) and 176.29(18)°, respectively. A similar bending of the Fe−C−O angles was also observed in $[Fe(PNP^{CH2}\text{-}tBu)(CO)_2]$.[17] The Fe−C bond distances in **7** are 1.719(2) and 1.737(2) Å for Fe1−C18 and Fe1−C19, respectively, which are similar to those in [Fe-

Scheme 5

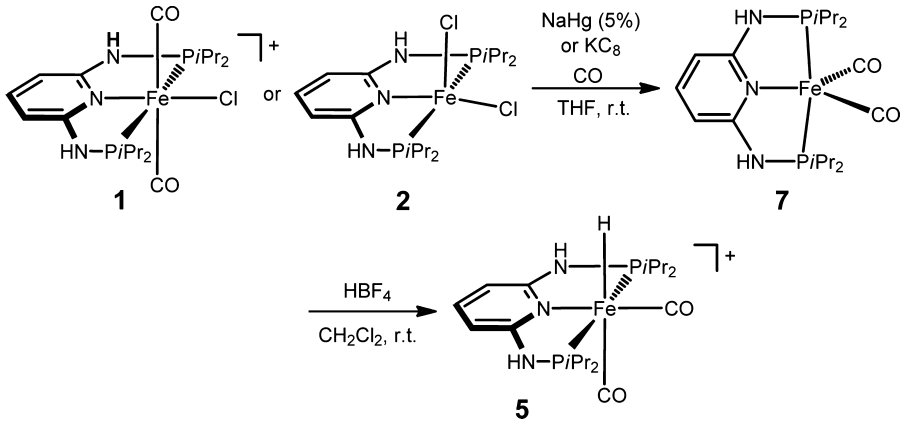

dx.doi.org/10.1021/om400241x | *Organometallics* 2013, 32, 4114−4121

Table 1. Selected Experimental and Calculated Bond Lengths and Angles of [Fe(PNP-*i*Pr)(CO)$_2$] (7) and [Fe(PNP^{CH2}-*i*Pr)(CO)$_2$]

	[Fe(PNP-*i*Pr)(CO)$_2$] (7)		[Fe(PNP^{CH2}-*i*Pr)(CO)$_2$]
	X-ray[a]	calcd	X-ray[b]
	Bond Lengths (Å)		
Fe1−N1/Fe2−N4	2.034(3)/2.032(3)	2.078	2.0684(8)
Fe1−C18/Fe2−C37	1.719(2)/1.745(3)	1.747	1.7325(9)
Fe1−C19/Fe2−C38	1.737(2)/1.755(3)	1.757	1.7325(9)
Fe1−P1/Fe2−P3	2.189(3)/2.172(3)	2.212	2.1941(2)
Fe1−P2/Fe2−P4	2.188(3)/2.178(3)	2.223	2.1941(2)
	Bond Angles (deg)		
Fe1−C18−O1/Fe2−C37−O3	175.47(15)/176.29(18)	175.4	174.84(11)
Fe1−C19−O2/Fe2−C38−O4	169.24(16)/172.72(15)	173.9	174.84(11)
C18−Fe1−C19/C37−Fe2−C38	113.88(9)/116.31(10)	117.0	119.91(7)
C18−Fe1−N1/C37−Fe2−N4	127.45(7)/129.48(8)	131.2	120.04(3)
C19−Fe1−N1/C38−Fe2−N4	118.67(7)/114.21(8)	111.7	120.04(3)
C18−Fe1−P1/C37−Fe2−P3	91.00(6)/92.34(6)	92.6	91.83(3)
C19−Fe1−P1/C38−Fe2−P3	97.09(6)/95.65(6)	95.6	91.83(3)
P1−Fe1−P2/P3−Fe2−P4	163.01(3)/162.57(3)	164.2	165.990(12)

[a]Two crystallographically independent complexes. [b]Reference 17.

(PNP^{CH2}-*i*Pr)(CO)$_2$] (1.7325(9) Å) and [Fe(PNP^{CH2}-*t*Bu)(CO)$_2$] (1.7310(12) and 1.7708(12) Å).

The calculated structure of **7** is in excellent agreement with the crystallographically determined structure, and selected bond distances and angles are provided in Table 1. These gas-phase DFT calculations also reproduce very well the Fe−C−O angles, and thus the bending seems to be not the result of crystal-packing effects.[17] The frontier orbitals of **7** are the expected ones for a trigonal-bipyramidal d^8 complex (TB),[20] with the five metal d orbitals split into the 2 + 2 + 1 set that would correspond to orbitals e″, e′, and a$_1$′ in a symmetrical complex (Figure 4). Thus, the first two orbitals (HOMO-4 and HOMO-2) are perpendicular to the equatorial plane (the N$_{py}$−C$_{CO}$−C$_{CO}$ plane) and correspond to the e″ set of a perfect TB complex; the following pair (HOMO and HOMO-1) is located on the equatorial plane and corresponds to e′ in a perfect TB geometry; finally, the least stable orbital (LUMO+3) corresponds to the z^2 orbital aligned with the axial ligands, the two P atoms, and it is the equivalent to a$_1$′ in a totally symmetric TB molecule.

Since Fe(0) complexes are known to undergo facile protonation at the metal center to afford Fe(II) hydride complexes,[21] protonation of **7** should constitute an alternative synthetic route to obtain complex **5**. As already expected from the shape and energy of the metal-centered HOMO (Figure 4), addition of HBF$_4$ to a CH$_2$Cl$_2$ solution of **7** resulted in an immediate color change from red to pale yellow consistent with protonation at the iron center to generate *cis*-[Fe(PNP-*i*Pr)(CO)$_2$H]$^+$ (**5**) in quantitative yield (Scheme 5), as established by NMR spectroscopy.

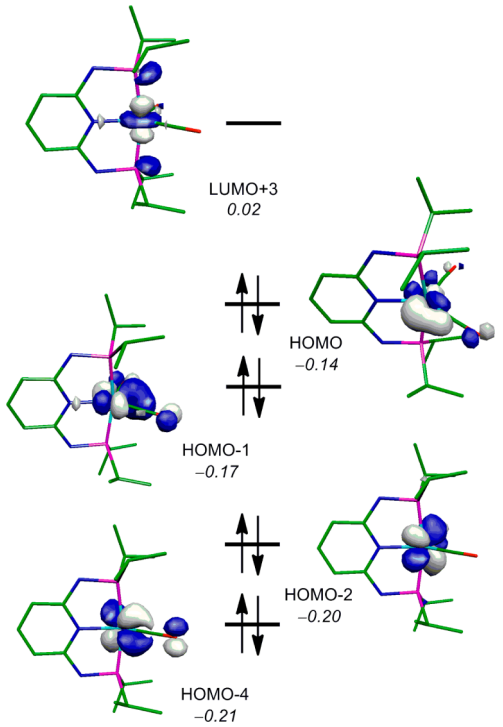

Figure 4. Frontier orbitals (d splitting) of [Fe(PNP-*i*Pr)(CO)$_2$] (**7**). H atoms are omitted for clarity, and the energy values (in au) are presented in italics.

CONCLUSION

We have developed two synthetic methodologies to obtain the Fe(II) hydride complex *cis*-[Fe(PNP-*i*Pr)(CO)$_2$H]$^+$ (**5**). The bis-carbonyl Fe(II) complex *trans*-[Fe(PNP-*i*Pr)(CO)$_2$Cl]$^+$ reacted with Zn as reducing agent under a dihydrogen atmosphere to give the Fe(II) hydride complex **5** in 97% isolated yield. Surprisingly, in the absence of H$_2$ the same complex was formed, albeit in only 40% yield. A crucial step in this reaction is the reduction of the acidic N−H protons of the PNP-*i*Pr ligand to release H$_2$ and to form the coordinatively unsaturated intermediate [Fe(PNP^H-*i*Pr)(CO)$_2$]$^+$, bearing a dearomatized pyridine moiety. This species is able to bind and heterolytically cleave H$_2$ to give **5**, where full aromatization of the pyridine moiety is re-established. This process is the rate-determining step. The mechanism of this reaction has been studied by DFT calculations, revealing that this activation process is facile with an overall barrier of 22.8 kcal/mol. The proposed mechanism was supported by deuterium-labeling experiments using D$_2$, where deuteride and N−D signals were observed in the ^{2}H NMR spectrum due to formation of the corresponding isotopologue of **5**. Moreover, the N-deuterated isotopologue *trans*-[Fe(PNP-*i*Pr)(CO)$_2$Cl]$^+$, featuring N−D

dx.doi.org/10.1021/om400241x | *Organometallics* 2013, 32, 4114−4121

instead of N−H moieties, did not afford **5** under the same reaction conditions, indicating a large kinetic isotope effect again supporting the involvement of NH in these reactions. Likewise, also the N-methylated *trans*-[Fe(PNP^{Me}-*i*Pr)-(CO)$_2$Cl]$^+$ did not react with Zn and H_2. An alternative synthesis of [Fe(PNP-*i*Pr)(CO)$_2$H]$^+$ was developed utilizing the Fe(0) complex [Fe(PNP-*i*Pr)(CO)$_2$]. This compound was obtained in high yield by treatment of either *trans*-[Fe(PNP-*i*Pr)(CO)$_2$Cl]$^+$ or [Fe(PNP-*i*Pr)Cl$_2$] with an excess of NaHg or stoichiometric amounts of KC_8 in the presence of carbon monoxide. [Fe(PNP-*i*Pr)(CO)$_2$] adopts a distorted-trigonal-bipyramidal structure. Interestingly, the Fe−C−O angles significantly deviate from linearity. Gas-phase DFT calculations reproduce very well the Fe−C−O angles, and thus the bending seems to be not the result of crystal-packing effects. Protonation of [Fe(PNP-*i*Pr)(CO)$_2$] with HBF_4 gave the hydride complex *cis*-[Fe(PNP-*i*Pr)(CO)$_2$H]$^+$ in high yield.

EXPERIMENTAL SECTION

General Considerations. All manipulations were performed under an inert atmosphere of argon by using Schlenk techniques or in a MBraun inert-gas glovebox. The solvents were purified according to standard procedures.[22] The deuterated solvents were purchased from Aldrich and dried over 4 Å molecular sieves. *trans*-[Fe(PNP-*i*Pr)(CO)$_2$Cl]SbF$_6$ (**1**), [Fe(PNP-*i*Pr)Cl$_2$] (**2**), [Fe(PNP^{Me}-*i*Pr)Cl$_2$] (**3**),[10a−c,11] and potassium graphite (KC_8)[23] were prepared according to the literature. ^{1}H, ^{2}H, ^{13}C{^{1}H}, and ^{31}P{^{1}H} NMR spectra were recorded on Bruker AVANCE-250 and AVANCE-300 DPX spectrometers. ^{1}H and ^{13}C{^{1}H} NMR spectra were referenced internally to residual protio solvent and solvent resonances, respectively, and are reported relative to tetramethylsilane (δ 0 ppm). ^{31}P{^{1}H} NMR spectra were referenced externally to H_3PO_4 (85%) (δ 0 ppm). ^{2}H NMR spectra were referenced to the deuterium resonance of extra added CD_2Cl_2 (δ 5.30 ppm).

***trans*-[Fe(PNP-*i*Pr)(CO)$_2$Cl]SbF$_6$ (1-d$_2$).** This complex was prepared in a fashion analogous to that for **1**[10c,d] utilizing the N-deuterated ligand PNP-*i*Pr. The latter was obtained by treatment of PNP-*i*Pr with D_2O in CH_2Cl_2. After drying over Na_2SO_4 and filtration under argon, the solvent was removed under vacuum, giving the N-deuterated ligand PNP-*i*Pr ligand in essentially quantitative yield.

***cis*-[Fe(PNP-*i*Pr)$_2$(CO)$_2$H]SbF$_6$ (5).** A solution of complex **1** (200 mg, 0.276 mmol) in THF (10 mL) was stirred in the presence of Zn powder (100 mg, 1.530 mmol) under a hydrogen atmosphere (1 bar) for 2 h. After that time the unreacted Zn powder was removed by filtration and the solution was filtrated through Celite. The solvent was evaporated under reduced pressure and the pale yellow solid was collected on a glass frit, washed with *n*-pentane, and dried under vacuum. Yield: 185 mg (97%). Anal. Calcd for $C_{19}H_{34}F_6FeN_3O_2P_2Sb$: C, 33.07; H, 4.97; N, 6.09. Found: C, 33.15; H, 4.86; N, 6.12. ^{1}H NMR (δ, CD_2Cl_2, 20 °C): 7.35 (t, 1H, J = 7.7 Hz, py^4), 6.78 (s, 2H, N*H*), 6.34 (d, 1H, J = 8.0, py^3), 2.90−2.20 (m, 4H, C*H*(CH$_3$)$_2$), 1.60−1.00 (m, 24H, CH(C*H*$_3$)$_2$), −7.47 (t, 1H, $^2J_{HP}$ = 47.7 Hz). ^{13}C{^{1}H} NMR (δ, CD_2Cl_2, 20 °C): 212.2 (t, J_{CP} = 20.2 Hz, CO), 207.5 (t, J_{CP} = 11.8 Hz, CO), 159.6 (t, J = 7.4 Hz, py^{2,6}), 140.7 (s, py^4), 99.3 (t, J = 2.4 Hz, py^{3,5}), 32.3 (t, J = 13.7 Hz, CH(CH$_3$)$_2$), 30.8 (t, J = 15.2 Hz, *C*H(CH$_3$)$_2$), 18.0 (s, CH(CH$_3$)$_2$), 17.9 (s, CH(CH$_3$)$_2$), 17.5 (s, CH(CH$_3$)$_2$), 17.2 (s, CH(CH$_3$)$_2$). ^{31}P{^{1}H} NMR (δ, CD_2Cl_2, 20 °C): 162.8. IR (ATR, cm^{-1}): 2027 (ν_{CO}), 1969 (ν_{CO}).

***trans*-[Fe(PNP^{Me}-*i*Pr)(CO)$_2$Cl]SbF$_6$ (6).** This complex was prepared analogously to **1** with **3** (250 mg, 0.504 mmol) and $AgSbF_6$ (173 mg, 0.504 mmol) as starting materials. Yield: 299 mg (82%). Anal. Calcd for $C_{21}H_{37}F_6FeN_3O_2P_2Sb$: C, 35.17; H, 5.20; N, 5.86. Found: C, 35.11; H, 5.24; N, 5.81. ^{1}H NMR (δ, CD_2Cl_2, 20 °C): 7.63 (bs, 1H, py^4), 6.22 (d, J = 7.6 Hz, 2H, py^{3,5}), 3.30 (bs, 4H, C*H*(CH$_3$)$_2$), 3.18 (bs, 6H, NC*H*$_3$), 1.60 (bs, 24H, CH(C*H*$_3$)$_2$). ^{13}C{^{1}H} NMR (δ, CD_2Cl_2, 20 °C): 211.5 (t, $^2J_{CP}$ = 24.1 Hz, CO), 163.0 (d, $^2J_{CP}$ = 7.2 Hz, py), 162.9 (d, $^2J_{CP}$ = 6.3 Hz, py), 142.1 (s, py^4), 100.0 (s, py^{3,5}), 35.3 (s, NCH$_3$), 32.0 (d, $^1J_{CP}$ = 11.1 Hz, *C*H(CH$_3$)$_2$), 31.9 (d, $^1J_{CP}$ = 11.0 Hz, *C*H(CH$_3$)$_2$), 18.5 (s, CH(CH$_3$)$_2$), 17.7 (s, CH(CH$_3$)$_2$). ^{31}P{^{1}H} NMR (δ, CD_2Cl_2, 20 °C): 130.7. IR (ATR, cm^{-1}): 2004 (ν_{CO}), 1980 (ν_{CO}).

[Fe(PNP-*i*Pr)$_2$(CO)$_2$] (7). Complex **2** (200 mg, 0.439 mmol) was added to a suspension of freshly prepared 5% Na/Hg (1.0 g, 2.174 mmol) in THF (10 mL), and CO was bubbled through the reaction mixture for 30 min, whereupon the solution changed from yellow to orange-red. The solution was decanted away from the amalgam and filtered through basic alumina. The filtrate was collected, and the solvent was removed under vacuum. Complex **7** was isolated as an orange solid. Yield: 88 mg (95%). Alternatively, complex **7** was also obtained in a similar yield by using 2.5 equiv of KC_8 (149 mg, 1.098 mmol) instead of Na/Hg as reducing reagent. The same reaction performed with **1** as starting material afforded similar yields. Anal. Calcd for $C_{19}H_{33}FeN_3O_2P_2$: C, 50.35; H, 7.34; N, 9.27. Found: C, 50.19; H, 7.40; N, 9.30. ^{1}H NMR (δ, THF-d_8, 20 °C): 6.97 (s, 2H, py^{3,5}), 6.86 (t, J = 7.1 Hz, 1H, py^4), 5.93 (d, J = 7.8 Hz, 2H, N*H*), 2.40 (s, 4H, C*H*(CH$_3$)$_2$), 1.28 (dd, J = 14.1, 6.8 Hz, 24H, CH(C*H*$_3$)$_2$). ^{13}C{^{1}H} NMR (δ, THF-d_8, −80 °C): 219.5 (t, J = 27.8 Hz, CO), 160.5 (s, py^{2,6}), 132.7 (s, py^4), 94.7 (s, py^{3,5}), 28.4 (d, J = 14.7 Hz, *C*H(CH$_3$)$_2$), 16.4 (d, J = 14.1 Hz; CH(CH$_3$)$_2$). ^{31}P{^{1}H} NMR (δ, THF-d_8, 20 °C): 173.8. IR (THF, cm^{-1}): 1842 (ν_{CO}), 1794 (ν_{CO}).

Reaction of [Fe(PNP-*i*Pr)$_2$(CO)$_2$] (7) with HBF$_4$. To a solution of **7** (80 mg, 0.181 mmol) in THF (10 mL) was added HBF_4 (24.3 μL, 0.181 mmol, 54% in Et_2O) at room temperature. After the solution was stirred for 1 h, solid materials were removed by filtration, and the solvent was evaporated under reduced pressure. The pale yellow solid (**5**) was collected on a glass frit, washed with *n*-pentane, and dried under vacuum. Yield: 88 mg (90%).

X-ray Structure Determination. X-ray diffraction data for **5** and **7**·CH_2Cl_2 were collected at T = 100 K on a Bruker Kappa APEX-2 CCD diffractometer with an Oxford Cryosystems cooler using graphite-monochromated Mo Kα radiation (λ = 0.71073 Å). A redundant data set was collected in φ- and ω-scan modes covering the whole reciprocal sphere. Data were reduced to intensity values with SAINT, and an absorption correction was applied with the multiscan approach implemented in SADABS.[24] The structures were solved by charge flipping using SUPERFLIP[25] and refined against F with JANA2006.[26] Non-hydrogen atoms were refined with anisotropic displacement parameters. The hydride and the N−H atoms could be unambiguously located in the difference Fourier maps. Details for **5**: the Fe−H distance was restrained to 1.46(2) Å. The H atoms of the ligands were placed at calculated positions and refined as riding on the parent atoms. The Sb atom of the SbF_6^- anion was refined as disordered around two positions with the occupation ratio 92.6:7.4(4). The highest peaks in the difference Fourier map of the final refinement cycles can be attributed to further unresolved disorder of the SbF_6^- anion. An attempt to model the disorder of the F atoms slightly improved reliability factors (R_{obs} = 0.047 vs 0.050) but resulted in an unreasonable geometry of the SbF_6^- anions and was therefore omitted from the final model. Details for **7**·CH_2Cl_2: one isopropyl group was modeled as disordered around two positions with an occupation ratio of 0.574:0.426(6). For one C atom the disorder could not be adequately resolved. It was therefore refined as a single position with enlarged ADPs. Molecular graphics were generated with the program MERCURY.[27] Crystal data and experimental details for **5** and **7**·CH_2Cl_2 are given in Table S1 (Supporting Information).

Computational Details. All calculations were performed using the GAUSSIAN 09 software package[28] on the Phoenix Linux Cluster of the Vienna University of Technology. The optimized geometries were obtained with the B3LYP functional.[29] That functional includes a mixture of Hartree−Fock[30] exchange with DFT[15] exchange correlation, given by Becke's three-parameter functional with the Lee, Yang, and Parr correlation functional, which includes both local and nonlocal terms. The basis set used for the geometry optimizations (basis b1) consisted of the Stuttgart/Dresden ECP (SDD) basis set[31] to describe the electrons of iron and a standard 6-31G** basis set[32] for all other atoms. Transition state optimizations were performed with the synchronous transit-guided quasi-Newton method (STQN) developed by Schlegel et al.,[33] following extensive searches of the

dx.doi.org/10.1021/om400241x | *Organometallics* 2013, 32, 4114−4121

potential energy surface. Frequency calculations were performed to confirm the nature of the stationary points, yielding one imaginary frequency for the transition states and none for the minima. Each transition state was further confirmed by following its vibrational mode downhill on both sides and obtaining the minima presented on the energy profiles. The electronic energies (E_{b1}) obtained at the B3LYP/b1 level of theory were converted to free energy at 298.15 K and 1 atm (G_{b1}) by using zero-point energy and thermal energy corrections based on structural and vibration frequency data calculated at the same level.

Single-point energy calculations were performed using the M06 functional and a standard 6-311++G(d,p) basis set,[34] on the geometries optimized at the B3LYP/b1 level. The M06 functional is a hybrid meta-GGA functional developed by Truhlar and Zhao,[35] and it was shown to perform very well for the kinetics of transition-metal molecules, providing a good description of weak and long-range interactions.[36] Solvent effects (THF) were considered in the M06/6-311G(d,p)//B3LYP/b1 energy calculations using the polarizable continuum model (PCM) initially devised by Tomasi and co-workers[37] with radii and nonelectrostatic terms of the SMD solvation model, developed by Truhler et al.[38]

The free energy values presented in the text (G_{b2}^{soln}) were derived from the electronic energy values obtained at the M06/6-311G(d,p)//B3LYP/b1 level, including solvent effects (E_{b2}^{soln}), according to the following expression: $G_{b2}^{soln} = E_{b2}^{soln} + G_{b1} - E_{b1}$. Three-dimensional representations of the orbitals were obtained with Molekel.[39]

■ ASSOCIATED CONTENT

Supporting Information

CIF files and a table giving complete crystallographic data for **5** and **7**·CH_2Cl_2 and tables giving atomic coordinates of all calculated structures. This material is available free of charge via the Internet at http://pubs.acs.org.

■ AUTHOR INFORMATION

Corresponding Author

*E-mail for K.K.: kkirch@mail.tuwien.ac.at.

Notes

The authors declare no competing financial interest.

■ ACKNOWLEDGMENTS

Financial support by the Austrian Science Fund (FWF) is gratefully acknowledged (Project No. P24583−N28). L.F.V. acknowledges UTL/Santander for partial fundin and Fundação para a Ciência e Tecnologia (FCT, project PEst-OE/QUI/UI0100/2011). The X-ray center of the Vienna University of Technology is acknowledged for providing access to the single-crystal diffractometer.

■ REFERENCES

(1) For reviews on pincer complexes, see: (a) Albrecht, M.; Van Koten, G. *Angew. Chem., Int. Ed.* **2001**, *40*, 3750−3781. (b) Van der Boom, M. E.; Milstein, D. *Chem. Rev.* **2003**, *103*, 1759−1792. (c) Singleton, J. T. *Tetrahedron* **2003**, *59*, 1837−1857. (d) Bhattacharya, P.; Guan, H. *Comment Inorg. Chem.* **2011**, *32*, 88−112. (e) Schneider, S.; Meiners, J.; Askevold, B. *Eur. J. Inorg. Chem.* **2012**, 412−429. (f) Morales-Morales, D., Jensen, C. M., Eds. *The Chemistry of Pincer Compounds*; Elsevier: Amsterdam, 2007. (g) Benito-Garagorri, D.; Kirchner, K. *Acc. Chem. Res.* **2008**, *41*, 201−213.

(2) For reviews on cooperative ligand effects, see: (a) Crabtree, R. H. *New J. Chem.* **2011**, *35*, 18−23. (b) Grützmacher, H. *Angew. Chem., Int. Ed.* **2008**, *47*, 1814−1818. (c) van der Vlugt, J. I.; Reek, J. N. H. *Angew. Chem., Int. Ed.* **2009**, *48*, 8832−8846.

(3) (a) Gunanathan, C.; D. Milstein, D. *Acc. Chem. Res.* **2011**, *44*, 588−602. (b) Gunanathan, C.; Milstein, D. *Top. Organomet. Chem.* **2011**, *37*, 55−84. (c) Milstein, D. *Top. Catal.* **2010**, *53*, 915−923. (d) Poverenov, E.; Milstein, D. *Top. Organomet. Chem.* **2013**, *40*, 21−47.

(4) For recent stoichiometric reactions involving PNP pincer complexes, see: (a) Vogt, M.; Gargir, M.; Iron, M. A.; Diskin-Posner, Y.; Ben-David, Y.; Milstein, D. *Chem. Eur. J.* **2012**, *18*, 9194−9197. (b) Vogt, M.; Rivada-Wheelaghan, O.; Iron, M. A.; Leitus, G.; Diskin-Posner, Y.; Shimon, L. J. W.; Ben-David, Y.; Milstein, D. *Organometallics* **2013**, *32*, 300−308. (c) Montag, M.; Zhang, J.; Milstein, D. *J. Am. Chem. Soc.* **2012**, *134*, 10325−10328. (d) Feller, M.; Diskin-Posner, Y.; Shimon, L. J. W.; Ben-Ari, E.; Milstein, D. *Organometallics* **2012**, *31*, 4083−4101.

(5) For recent catalytic reactions involving PNP pincer complexes, see: (a) Balaraman, E.; Khaskin, E.; Leitus, G.; Milstein, D. *Nature Chem.* **2013**, *5*, 122−125. (b) Srimani, D.; Feller, M.; Ben-David, Y.; Milstein, D. *Chem. Commun.* **2012**, *48*, 11853−11855. (c) Srimani, Balaraman, E.; Gnanaprakasam, B.; Ben-David, Y.; Milstein, D. *Adv. Synth. Catal.* **2012**, *354*, 2403−2406. (d) Kossoy, E.; Diskin-Posner, Y.; Leitus, G.; Milstein, D. *Adv. Synth. Catal.* **2012**, *354*, 497−504. (e) Schwartsburd, L.; Iron, M. A.; Konstantinowski, L.; Ben-Ari, E.; Milstein, D. *Organometallics* **2011**, *30*, 2721−2729.

(6) For iron PNP complexes, see: (a) Langer, R.; Iron, M. A.; Konstantinovski, L.; Diskin-Posner, Y.; Leitus, G.; Ben-David, Y.; Milstein, D. *Chem. Eur. J.* **2012**, *18*, 7196−7209. (b) Langer, R.; Leitus, G.; Ben-David, Y.; Milstein, D. *Angew. Chem., Int. Ed.* **2011**, *50*, 2120−2124. (c) Langer, R.; Diskin-Posner, Y.; Leitus, G.; Shimon, L. J.; Ben-David, Y.; Milstein, D. *Angew. Chem., Int. Ed.* **2011**, *50*, 9948−9952.

(7) (a) Maire, P.; Buttner, T.; Breher, F.; Le Floch, P.; Grützmacher, H. *Angew. Chem., Int. Ed.* **2005**, *44*, 6318−6323. (b) Ohkuma, T.; Utsumi, N.; Tsutsumi, K.; Murata, K.; Sandoval, C.; Noyori, R. *J. Am. Chem. Soc.* **2006**, *128*, 8724−8725. (c) Phillips, A. D.; Laurenczy, G.; Scopelliti, R.; Dyson, P. J. *Organometallics* **2007**, *26*, 1120−1122. (d) Friedrich, A.; Drees, M.; auf der Gunne, J. S.; Schneider, S. *J. Am. Chem. Soc.* **2009**, *131*, 17552−17553. (e) Kass, M.; Friedrich, A.; Drees, M.; Schneider, S. *Angew. Chem., Int. Ed.* **2009**, *48*, 905−907. (f) Picot, A.; Dyer, H.; Buchard, A.; Auffrant, A.; Vendier, L.; Le Floch, P.; Sabo-Etienne, S. *Inorg. Chem.* **2010**, *49*, 1310−1312. (g) Misumi, Y.; Seino, H.; Mizobe, Y. *J. Am. Chem. Soc.* **2009**, *131*, 14636−14637. (h) Cheung, F. K.; Clarke, A. J.; Clarkson, G. J.; Fox, D. J.; Graham, M. A.; Lin, C. X.; Criville, A. L.; Wills, M. *Dalton Trans.* **2010**, *39*, 1395−1402. (i) He, T.; Tsvetkov, N. P.; Andino, J. G.; Gao, X.; Fullmer, B. C.; Caulton, K. G. 2010, *132*, 910−911. (j) Mastrorilli, P.; Latronico, M.; Gallo, V.; Polini, F.; Re, N.; Marrone, A.; Gobetto, R.; Ellena, S. *J. Am. Chem. Soc.* **2010**, *132*, 4752−4765. (k) Stepowska, E.; Huiling Jiang, H.; Song, D. *Chem. Commun.* **2010**, *46*, 556−558. (l) Bertoli, M.; Choualeb, A.; Gusev, D. G.; Lough, A. J.; Major, Q.; Moore, B. *Dalton Trans.* **2011**, *40*, 8941−8949. (m) Hoyle, M. M.; Pantazis, D. A.; Burton, H. M. †; Robert McDonald, R.; Rosenberg, L. *Organometallics* **2011**, *30*, 6458−6465. (n) Liu, T.; Chen, S.; O'Hagan, M. J.; DuBois, M. R.; Bullock, R. M.; DuBois, D. L. *J. Am. Chem. Soc.* **2012**, *134*, 6257−6272. (o) Wylie, W. N. O.; Lough, A. J.; Morris, R. H. *Organometallics* **2012**, *31*, 2137−2151.

(8) Benito-Garagorri, D.; Becker, E.; Wiedermann, J.; Lackner, W.; Pollak, M.; Mereiter, K.; Kisala, J.; Kirchner, K. *Organometallics* **2006**, *25*, 1900−1913.

(9) Benito-Garagorri, D.; Mereiter, K.; Kirchner, K. *Eur. J. Inorg. Chem.* **2006**, 4374−4379.

(10) For related iron PNP complexes, see: (a) Benito-Garagorri, D.; Wiedermann, J.; Pollak, M.; Mereiter, K.; Kirchner, K. *Organometallics* **2007**, *26*, 217−222. (b) Benito-Garagorri, D.; Puchberger, M.; Mereiter, K.; Kirchner, K. *Angew. Chem., Int. Ed.* **2008**, *47*, 9142−9145. (c) Benito-Garagorri, D.; Alves, L. G.; Puchberger, M.; Mereiter, K.; Veiros, L. F.; Calhorda, M. J.; Carvalho, M. D.; Ferreira, L. P.; Godinho, M.; Kirchner, K. *Organometallics* **2009**, *28*, 6902−6914. (d) Benito-Garagorri, D.; Alves, L. G.; Veiros, L. F.; Standfest-Hauser, C. M.; Tanaka, S.; Mereiter, K.; Kirchner, K. *Organometallics* **2010**, *29*, 4932−4942.

(11) Öztopcu, Ö.; Holzhacker, C.; Puchberger, M.; Weil, M.; Mereiter, K.; Veiros, L. F.; Kirchner, K. *Organometallics* **2013**, *32*, 3042−3052.

(12) He, L.-P.; Chen, T.; Xue, D.-X.; Eddaoudi, M.; Huang, K.-W. *J. Organomet. Chem.* **2012**, *700*, 202−206.
(13) Qantitative isomerization of **1** (in the form of its BAr'_4^- salt (Ar′ = 3,5-$C_6H_3(CF_3)_2$)) to **4** took place in CH_2Cl_2 as solvent if kept in the dark for several days at room temperature. On exposure to visible light complex **1** was re-formed within 3 h.
(14) For large kinetic isotope effects in proton-coupled electron transfer processes see: Huynh, H. V.; Meyer, T. J. *Proc. Natl. Acad. Sci. U.S.A.* **2004**, *101*, 13138−13141.
(15) Parr, R. G.; Yang, W. *Density Functional Theory of Atoms and Molecules*; Oxford University Press: New York, 1989.
(16) Taken as the angle between the mean plane defined by the six atoms of the pyridine ring and the plane defined by the FePNP frame.
(17) Trovitch, R. J.; Lobkovsky, E.; Chirik, P. J. *Inorg. Chem.* **2006**, *45*, 7252−7260.
(18) Jaunky, P.; Schmalle, H. W.; Blacque, O.; Fox, T.; Berke, H. *J. Organomet. Chem.* **2005**, *690*, 1429−1455.
(19) For a discussion of bent CO ligands, see: Pelczar, E. M.; Emge, T. J.; Krogh-Jespersen, K.; Goldman, A. S. *Organometallics* **2008**, *27*, 5759−5767.
(20) Albright, T. A.; Burdett, J. K.; Whangbo, M. H. *Orbital Interactions in Chemistry*; Wiley: New York, 1985; pp 310−326.
(21) Li, T.; Lough, A. J.; Morris, R. H. *Chem. Eur. J.* **2007**, *13*, 3796−3803.
(22) Perrin, D. D.; Armarego, W. L. F. *Purification of Laboratory Chemicals*, 3rd ed.; Pergamon: New York, 1988.
(23) Weitr, I. S.; Rabinovitz, M. *J. Chem. Soc., Perkin Trans. 1* **1993**, *1*, 117−120.
(24) Bruker computer programs: *APEX2, SAINT and SADABS*; Bruker AXS Inc., Madison, WI, 2012.
(25) Palatinus, L.; Chapuis, G. *J. Appl. Crystallogr.* **2007**, *40*, 786−790.
(26) Petříček, V.; Dušek, M.; Palatinus, L. *JANA2006, the crystallographic computing system*; Institute of Physics, Praha, Czeck Republic, 2006.
(27) Macrae, C. F.; Edgington, P. R.; McCabe, P.; Pidcock, E.; Shields, G. P.; Taylor, R.; Towler, M.; van de Streek, J. *J. Appl. Crystallogr.* **2006**, *39*, 453−457.
(28) Frisch, M. J. et al. *Gaussian 09, Revision A.02*; Gaussian, Inc., Wallingford, CT, 2009.
(29) (a) Becke, A. D. *J. Chem. Phys.* **1993**, *98*, 5648−5652. (b) Miehlich, B.; Savin, A.; Stoll, H.; Preuss, H. *Chem. Phys. Lett.* **1989**, *157*, 200−206. (c) Lee, C.; Yang, W.; Parr, G. *Phys. Rev. B* **1988**, *37*, 785−789.
(30) Hehre, W. J.; Radom, L.; Schleyer, P. v. R.; Pople, J. A. *Ab Initio Molecular Orbital Theory*; Wiley: New York, 1986.
(31) (a) Haeusermann, U.; Dolg, M.; Stoll, H.; Preuss, H. *Mol. Phys.* **1993**, *78*, 1211−1224. (b) Kuechle, W.; Dolg, M.; Stoll, H.; Preuss, H. *J. Chem. Phys.* **1994**, *100*, 7535−7542. (c) Leininger, T.; Nicklass, A.; Stoll, H.; Dolg, M.; Schwerdtfeger, P. *J. Chem. Phys.* **1996**, *105*, 1052−1059.
(32) (a) McLean, A. D.; Chandler, G. S. *J. Chem. Phys.* **1980**, *72*, 5639−5648. (b) Krishnan, R.; Binkley, J. S.; Seeger, R.; Pople, J. A. *J. Chem. Phys.* **1980**, *72*, 650−654. (c) Wachters, A. J. H. *J. Chem. Phys.* **1970**, *52*, 1033−1036. (d) Hay, P. J. *J. Chem. Phys.* **1977**, *66*, 4377−4384. (e) Raghavachari, K.; Trucks, G. W. *J. Chem. Phys.* **1989**, *91*, 1062−1065. (f) Binning, R. C., Jr.; Curtiss, L. A. *J. Comput. Chem.* **1990**, *11*, 1206. (g) McGrath, M. P.; Radom, L. *J. Chem. Phys.* **1991**, *94*, 511−516.
(33) (a) Peng, C.; Ayala, P. Y.; Schlegel, H. B.; Frisch, M. J. *J. Comput. Chem.* **1996**, *17*, 49−56. (b) Peng, C.; Schlegel, H. B. *Isr. J. Chem.* **1993**, *33*, 449−454.
(34) (a) McClean, A. D.; Chandler, G. S. *J. Chem. Phys.* **1980**, *72*, 5639−5648. (b) Krishnan, R.; Binkley, J. S.; Seeger, R.; Pople, J. A. *J. Chem. Phys.* **1980**, *72*, 650−654. (c) Wachters, A. J. H. *J. Chem. Phys.* **1970**, *52*, 1033−1036. (d) Hay, P. J. *J. Chem. Phys.* **1977**, *66*, 4377−4384. (e) Raghavachari, K.; Trucks, G. W. *J. Chem. Phys.* **1989**, *91*, 1062−1065. (f) Binning, R. C., Jr.; Curtiss, L. A. *J. Comput. Chem.* **1990**, *11*, 1206−1216. (g) McGrath, M. P.; Radom, L. *J. Chem. Phys.* **1991**, *94*, 511−516. (h) Clark, T.; Chandrasekhar, J.; Spitznagel, G. W.; Schleyer, P. v. R. *J. Comput. Chem.* **1983**, *4*, 294−301. (i) Frisch, M. J.; Pople, J. A.; Binkley, J. S. *J. Chem. Phys.* **1984**, *80*, 3265−3269.
(35) Zhao, Y.; Truhlar, D. G. *Theor. Chem. Acc.* **2008**, *120*, 215−241.
(36) (a) Zhao, Y.; Truhlar, D. G. *Acc, Chem. Res.* **2008**, *41*, 157−167. (b) Zhao, Y.; Truhlar, D. G. *Chem. Phys. Lett.* **2011**, *502*, 1−13.
(37) (a) Cancès, M. T.; Mennucci, B.; Tomasi, J. *J. Chem. Phys.* **1997**, *107*, 3032−3041. (b) Cossi, M.; Barone, V.; Mennucci, B.; Tomasi, J. *Chem. Phys. Lett.* **1998**, *286*, 253−260. (c) Mennucci, B.; Tomasi, J. *J. Chem. Phys.* **1997**, *106*, 5151−5158. (d) Tomasi, J.; Mennucci, B.; Cammi, R. *Chem. Rev.* **2005**, *105*, 2999−3094.
(38) Marenich, A. V.; Cramer, C. J.; Truhlar, D. G. *J. Phys. Chem. B* **2009**, *113*, 6378−6396.
(39) Portmann, S.; Lüthi, H. P. *Chimia* **2000**, *54*, 766−770.